

Introduction

The oceans underwent some of the most remarkable transformations in Earth's history in the Neoproterozoic, such as the appearance of animal life (Knoll, 2015), major excursions in sulphur and carbon isotope records (Kaufman and Knoll, 1995; Halverson and Hurtgen, 2007) and indications of a transition from an anoxic to a partially oxygenated deeper ocean in the aftermath of the Marinoan glaciation (Planavsky *et al.*, 2010). These changes can arguably be best studied in marine sediments from the Yangtze Platform, South China, that cover the critical time span from the Cryogenian to the Precambrian-Cambrian (PCC) boundary which saw the appearance of the first macroscopic fossils (*e.g.*, Yin *et al.*, 2007). For this reason, it may also be an ideal place to evaluate whether Cd isotopes in marine sediments can be used as a palaeo-productivity proxy. To test this, we analysed shallow-water carbonates from the Ediacaran Xiaofenghe section that was deposited on the S-SE-facing passive margin of the Yangtze Craton and hosts abundant fossil assemblages of multicellular life from the Doushantuo and Dengying Formations (Xiao *et al.*, 2012).

Stable isotope fractionation of Cd is a new proxy for studying biogeochemical cycling of micronutrients in the present-day oceans (Lacan *et al.*, 2006; Ripperger *et al.*, 2007; Abouchami *et al.*, 2011) and in sedimentary archives, such as Fe-Mn crusts (Schmitt, *et al.*, 2009; Horner *et al.*, 2010). Seawater profiles of Cd show a nutrient-like behaviour, with strong near-surface depletions and deep-water enrichments, mimicking profiles of macronutrient phosphate (Boyle *et al.*, 1976). The surface depletions in Cd are associated with "heavier" Cd stable isotopic compositions, which are thought to be due to preferential uptake of the "lighter" isotopes during incorporation of Cd by phytoplankton (Lacan *et al.*, 2006; Ripperger *et al.*, 2007; Abouchami *et al.*, 2011). At the moment, there is no general understanding of why cadmium, which is toxic to most life, should be taken up. Zinc is required by all organisms and in the case of phytoplankton is the cofactor in zinc carbonic anhydrase (Zn-CA), an enzyme involved in photosynthesis. Under zinc-poor conditions, Cd can substitute for Zn in Zn-CA and, furthermore, Price and Morel (1990) have described a cadmium-bearing carbonic anhydrase variant (Cd-CA) with the same functionality; but Cd-CA is only known from a few diatom species (Park *et al.*, 2007) whose first appearance lies in the Mesozoic. Studying Cd systematics in Proterozoic sediments could therefore possibly provide insights into the lineage of the CA enzymes. It is equally possible that cadmium fulfills no biological role at all, in most cases, and that Cd uptake is driven by absorption onto organic matter or that Cd is pumped into the cell through the membrane, mistaken for Zn.

Similarly, it remains unclear what the precise mechanism is for causing the isotopic fractionation of Cd during uptake from seawater. Pure inorganic absorption (Wasylenki *et al.*, 2014), partitioning into calcite (Horner *et al.*, 2011) and biological utilisation are known to favour the light isotopes, which would all be consistent with the observation of heavy Cd in surface seawaters. But irrespective of these uncertainties concerning the reason for uptake and site of fractionation,

Cadmium isotope variations in Neoproterozoic carbonates – A tracer of biologic production?

S.V. Hohl^{1,2*}, S.J.G. Galer³, A. Gamper⁴, H. Becker¹



doi: 10.7185/geochemlet.1704

Abstract

Cadmium concentrations and stable isotopic compositions in seawater are important tools for studying the biogeochemical cycling of Cd in the modern oceans and as a proxy for micronutrient utilisation by phytoplankton. It is now well established that Cd isotopes become "heavier" as the primary production in the surface ocean increases, even though the mechanism driving the isotopic fractionation is still debated. Here, we use this property of Cd isotopes to examine changes that took place in the oceans during the emergence of multicellular life in the Neoproterozoic. Isotopic compositions and concentrations of Cd, N and C are reported in shallow-water carbonates of Ediacaran age from the Xiaofenghe section on the Yangtze Platform, South China. The Cd isotope data - reported as $\epsilon^{112/110}\text{Cd}$ - show positive excursions in the cap dolomites, while significantly lighter Cd is found in the overlying strata. After correction for salinity-controlled fractionation into inorganic calcite, calculated palaeo-seawater $\epsilon^{112/110}\text{Cd}_{\text{sw}}$ range from -2 to +1.5, overlapping values of modern surface seawater. Importantly, $\epsilon^{112/110}\text{Cd}_{\text{sw}}$ and $\delta^{13}\text{C}$ show a general positive correlation, as would be expected in bio-productive environments. However, the trend to lighter $\epsilon^{112/110}\text{Cd}$ up-section is not that explicitly expected for an "explosion of life" at the end of the Ediacaran. The upper Doushantuo also displays substantial fluctuations in REE abundances, $\delta^{15}\text{N}$ and $\delta^{13}\text{C}$, which may be due to estuarine mixing. Our data suggest that the variations in $\epsilon^{112/110}\text{Cd}$ are a result of biologically-induced fractionation in at least some of the Ediacaran carbonates at Xiaofenghe. Further Cd isotope fractionation processes are clearly playing a role as well, such as precipitation of sulphides under anoxic pore-water conditions and fractionation into inorganic carbonates under variable salinity conditions. These effects have to be evaluated carefully when using Cd isotope systematics in ancient marine carbonates to look for palaeo-productivity signals.

Received 19 May 2016 | Accepted 31 August 2016 | Published 9 September 2016

1. Institut für Geologische Wissenschaften, Freie Universität Berlin, Germany
2. State Key Laboratory for Mineral Deposits Research, Department of Earth Sciences, Nanjing University, Nanjing, China
- * Corresponding author (email: shohl@zedat.fu-berlin.de)
3. Max-Planck-Institut für Chemie, Abteilung Klimageochemie, Mainz, Germany
4. Museum für Naturkunde Berlin, Leibniz Institute for Evolution and Biodiversity Science, Berlin, Germany



Cd isotopes can be used as a convincing proxy for productivity in surface waters in the sense that the greater the depletion in Cd (and macronutrients like phosphate), the isotopically heavier the Cd becomes that is left behind in seawater.

So far the oldest sediments analysed for their Cd isotopic compositions are Permian in age (Georgiev *et al.*, 2015). Studying Cd isotopes in our Ediacaran-age carbonates could potentially document palaeo-seawater biogeochemical cycling of cadmium, providing insights into evolution of multicellular life at the PCC boundary. Furthermore, Cd isotopes may also be used to support interpretations from other bio-available isotopic tracers. In recent years, $\delta^{15}\text{N}$ has provided important insights into palaeo-ocean nutrient-cycling and redox conditions (Ader *et al.*, 2014). As the $\delta^{15}\text{N}$ proxy is often affected by post-depositional modification (Bebout and Fogel, 1992), combining with Cd isotopes is potentially useful in screening such datasets. Nevertheless, when analysing Cd isotopes in ancient sediments, other factors that may mask the true seawater signal must be carefully evaluated, such as fluid flow alteration and additional inorganic fractionation processes (*e.g.*, variable salinity, authigenic sulphide precipitation).

Results and Discussion

Stable isotope measurements of C and N were performed on carbonates and bulk rock using standard methods. Stable Cd isotope compositions on acetic acid leachates from alteration-free carbonates were determined using a double-spike method and TIMS (see Schmitt *et al.*, 2009; Abouchami *et al.*, 2011; detailed analytical protocols in Supplementary Information).

The $\delta^{13}\text{C}_{\text{org}}$ values obtained up the stratigraphic section remain relatively constant at -28‰ before decreasing to -34‰ in black shales of the middle Doushantuo, where TOC values increase to 1.1%. These values are characteristic of enhanced planktonic productivity and remineralisation and resemble previously published data from the Doushantuo (*e.g.*, Ishikawa *et al.*, 2013). In the cap dolostones $\delta^{13}\text{C}_{\text{org}}$ and $\delta^{13}\text{C}_{\text{carb}}$ are decoupled ($\Delta^{13}\text{C} = 25$ vs. 33 in overlying strata, Fig. 1c) and this is mimicked in a shift in average bulk $\delta^{15}\text{N}$ values from $+1.6\text{‰}$ to $+4.2\text{‰}$ (Fig. 1f), possibly indicating a change in the nutrient regime to a NO_3^- -dominated marine environment (Ader *et al.*, 2014). In the Doushantuo Formation, nitrate presumably became the main utilised nutrient for primary producers while N_2 partly remained unused in surface-waters, where incomplete denitrification shifts seawater to higher $\delta^{15}\text{N}$. This may possibly be attributable to increased oxygen availability, which is essential for organic matter (OM) remineralisation via nitrification-denitrification (Canfield *et al.*, 2010); however, smaller second-order variations in the $\delta^{15}\text{N}$ curve might simply be due to alteration.

Cadmium isotopic compositions in carbonates vary by more than four $\epsilon^{112/110}\text{Cd}$ units and show no definite correlation with Cd (Fig. 2a) nor K concentrations (see Fig. S-1b). Cadmium concentrations in detrital material are very

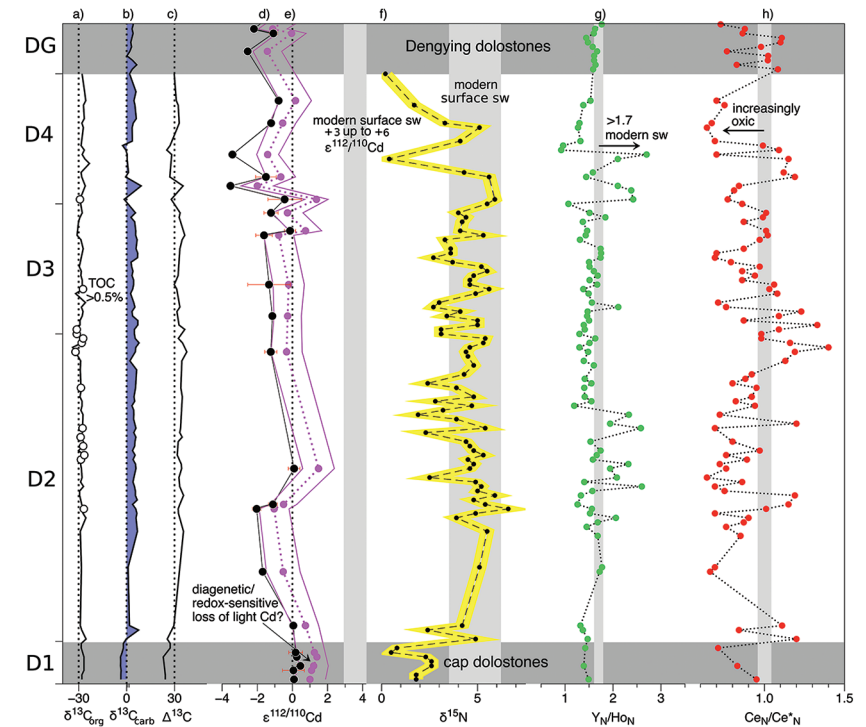


Figure 1 Isotope and concentration data from Xiaofenghe section. Samples are drawn in equidistance according to their sample numbers in Table 1 for better visibility. (a-c) Carbon isotope data. (d) Carbonate $\epsilon^{112/110}\text{Cd}$ (error bars = 2σ), grey bar = discrimination line for modern seawater values (Ripperger *et al.*, 2007). (e) Salinity-corrected $\epsilon^{112/110}\text{Cd}$ of seawater. (f) Bulk $\delta^{15}\text{N}$, yellow envelope = 0.2‰ uncertainty, grey bar = modern surface water. (g, h) Shale-normalised Y/Ho and Ce/Ce* in carbonates, grey bars represents discrimination of modern seawater values (Bau *et al.*, 1995) and negative/positive Ce anomalies.

low, so the effect of detrital input on $\epsilon^{112/110}\text{Cd}$ is likely negligible in extent. Late fluid-flow overprint is typical for many Neoproterozoic carbonates and may also have altered the Cd isotope signatures. However, Hohl *et al.* (2015) have shown that, with the exception of the cap dolostones, carbonates at Xiaofenghe were not much affected by fluids (SEM pre-screening, no co-variation of $\delta^{18}\text{O}$ with $^{87}\text{Sr}/^{86}\text{Sr}$ or Mn/Sr); thus, their trace element budgets and isotopic compositions most likely reflect partitioning and incorporation from Ediacaran seawater. In the cap dolostones $\epsilon^{112/110}\text{Cd} > 0$, while low Cd and N concentrations (Fig. S-1d) correlate with light $\delta^{13}\text{C}_{\text{carb}}$ (Fig. 1c) and high Mn/Sr ratios (see Fig. S-1a), commonly used as indicators of fluid overprinting (Brand and Veizer, 1980).



Table 1 Stable isotope data; N and C concentrations; assorted shale normalised REE ratios and Mn enrichments relative to Cal-5 from Hohl et al. (2015b). D1-D4 = Doushantuo Fm., DG = Dengying Fm.

sample	Height [m]	Member	$\delta^{13}\text{C}_{\text{carb}}^1$	$\delta^{18}\text{O}_{\text{carb}}^1$	$\delta^{13}\text{C}_{\text{org}}$	$\Delta\delta^{13}$	$\epsilon^{112/110}\text{Cd}^2$	2SE	Cd [$\mu\text{g/g}$]
1	0.2	D1	-3.8	-6.7	-28	24.2	0.09	0.2	0.06
2	0.75	D1			-26.7		0.06	0.62	0.1
3	1.6	D1	-3.7	-7.7			0.46	0.23	0.03
4	2.3	D1	-3.8	-7.3	-26.7	22.9	0.25	0.19	0.07
5	3.85	D1	-3.2	-6.9			0.18	0.39	0.03
6	4.8	D1	-1.2	-12.3	-28.4	27.2			
7	6.65	D2	0.0	-6.8	-25.4	25.4			
8	12.1	D2			-28.1				
9	22	D2	0.6	-10.4	-29	29.6	1.07	0.35	0.03
10	36	D2					-1.69	0.09	0.2
11	37.5	D2			-28.3				
12	65	D2	6.5	-6.1	-29	35.5			
13	73.7	D2			-25.5				
14	75	D2	5.1	-4.8	-27.3	32.4			
15	75.6	D2	5.4	-4.4	-26.8	32.2	-2.04	0.25	0.04
16	76	D2	5.2	-4.5	-28.1	33.3	-1.11	0.25	0.05
17	76.5	D2							
18	77.5	D2	6.2	-4.1	-29.4	35.6			
19	77.5	D2			-29.4				
20	79.5	D2	6.2	-4.1	-27	33.2			
21	80.5	D2			-28.8				
22	81.5	D2	4.8	-5.0	-27.9	32.7			
23	84.5	D2	6.1	-1.6	-28.3	34.4	0.1	0.33	0.02
24	85	D2	5.4	-4.4	-28.8	34.2			
25	86	D2			-28.6				
26	87.2	D2	5.2	-3.9	-26.5	31.7			
27	88	D2			-30.1				
28	88.7	D2			-27.2				
29	89	D2	5.2	-4.0	-27	32.2			
30	91.2	D2	5.5	-3.3	-27.7	33.2			
31	91.7	D2	6.1	-2.9	-27.6	33.7			
32	92.5	D2							
33	93	D2			-27.3				
34	96.2	D2			-28.6				
35	98	D2			-27.9				
36	99	D2			-27.9				
37	99.85	D2	5.6	-2.6	-29.2	34.8			
38	101.5	D2	5.3	-3.4	-28.6	33.9			
39	101.85	D2	5.8	-2.4					
40	102	D2	6.3	-1.3					
41	102.4	D2							
42	102.6	D2							
43	102.7	D2	5.6	-1.5	-32	37.6	-1.23	0.35	0.1

¹ O and C isotopic data relative to VPDB; ² Cd relative to NIST SRM 3108; ³ N relative to Air; ⁴ calculated following equations given by Lawrence and Kamber, 2006.

$\delta^{15}\text{N}^3$	N [wt. %]	TOC [wt.%]	C/N	ΣREE [$\mu\text{g/g}$]	Ce/Ce* ⁴	$\text{Y}_\text{N}/\text{Ho}_\text{N}$	$\text{Pr}_\text{N}/\text{Yb}_\text{N}$	EF $\text{Mn}_{(\text{Cal-S})}$
1.8	0.003	0.01	2.7	16	0.95	1.5	0.97	48
		0.11						
2.6	0.006			27	0.83	1.4	1.1	30
2.3	0.005	0.0001	0.02					
0.5	0.011							
0.8	0.004	0.06	15	2.1	0.71	1.4	0.97	1
4.9	0.066	0.02	0.2	13	1.2	1.5	1.05	496
2.4	0.008	0.25	32	4.9	0.84	1.4	0.85	7.8
4.2	0.011	0.12	11	2.5	1.11	1.3	0.41	8.9
				2.2	0.66	1.7	0.57	2.1
5.1	0.014	0.21	15	1.7	0.69	1.8	0.49	2.9
5.5	0.028	0.12	4.4	0.33				0.71
3.9	0.017			3.8	0.9	2.1	0.77	6.4
4.9	0.092			0.33	0.69	1.5	0.4	0.14
6.6	0.13	0.61	4.7	2.9	1.01	1.6	0.58	1.7
5.4	0.034	0.22	6.6	2.9	1.15	1.3	0.62	5.2
4.8	0.023							
5.9	0.046	0.43	9.3	3.4	1.19	1.3	0.63	5.2
5.0	0.032	0.42	13	1.4	0.75	1.6	0.49	4.8
5.2	0.044	0.41	9.4	1.7	0.69	2.6	0.37	1.7
4.9	0.049	0.38	7.7	13	0.86	1.4	1.31	3.8
2.5	0.092	0.01	0.1	3.2	0.64	2.1	0.5	1.6
4.6	0.031	0.45	14	3.6	0.76	1.9	0.65	2.2
4.8	0.034	0.48	14	1.9	0.72	2.3	0.36	2.5
4.5	0.067	0.92	14	6.4	0.89	1.6	0.81	2.1
5.3	0.044	0.71	16	6.9	0.76	1.7	0.89	2.5
4.8	0.037	0.36	10	7.3	0.97	1.7	0.7	2.2
4.6	0.048	0.71	15					
4.4	0.044			6.7	0.8	1.5	0.91	1.1
2.3	0.017	0.29	17					
5.4	0.087	0.77	8.9	1.3	0.69	2.58	0.49	2.3
3.9	0.020							
1.9	0.011	0.26	23	2.4	0.72	2.3	0.57	1.4
3.2	0.014	0.35	25					
4.7	0.04	0.35	8.7	29	0.94	1.2	0.92	3.2
2.8	0.011	0.15	13	16	0.82	1.6	1.52	3.1
4.8	0.06	0.32	5.3	10	0.92	1.4	1.36	2.9
3.9	0.019	0.65	34	3.5	0.95	1.4	0.82	3.6
2.4	0.017	0.28	16	6	0.8	1.6	1.22	4
4.3	0.045			9.4	0.92			2.5
4.8	0.094	0.95	10			1.6	0.8	
4.5	0.097	0.4	4.1				0.63	
4.4	0.085	1	12	5.8	1.19	1.5	0.73	4.0



sample	Height [m]	Member	$\delta^{13}\text{C}_{\text{carb}}^1$	$\delta^{18}\text{O}_{\text{carb}}^1$	$\delta^{13}\text{C}_{\text{org}}$	$\Delta\delta^{13}$	$\varepsilon^{112/110}\text{Cd}^2$	2SE	Cd [$\mu\text{g/g}$]
44	103	D2			-33.8				
45	103	D2	6.8	-1.1	-28.1	34.9			
46	103	D2	5.1	-2.1	-27.2	32.3			
47	103.5	D3			-31.2				
48	103.5	D3	5.2	-3.4	-31.2	36.4			
49	104	D3	3.5	-2.8	-29.2	32.7			
50	104	D3			-29.2				
51	104.25	D3			-27.8		-1.14	0.12	0.4
52	104.5	D3	4.2	-2.2	-27.3	31.5			
53	104.5	D3	5.0	-4.9	-28.3	33.3			
54	105.5	D3			-25.8				
55	108.15	D3			-31.9				
56	108.7	D3	4.0	-1.0	-27.3	31.3			
57	109.5	D3	2.0	-6.3	-27.8	29.8	-1.33	1.21	0.03
58	109.5	D3			-27.8				
59	110	D3	3.6	-6.8	-28.6	32.2			
60	110.5	D3			-28.4				
61	111.1	D3	2.9	-6.8	-29.6	32.5			
62	112.2	D3	2.8	-8.6					
63	113.9	D3	6.6	-5.4					
64	116	D3	6.9	-4.6					
65	118.5	D3	6.1	-6.4	-27.2	33.3			
66	123.8	D3	6.1	-2.3	-28.6	34.7			
67	125	D3	5.4	-3.2	-31	36.4	-1.62	0.47	0.02
68	130	D3	5.7	-4.9			-0.13	0.31	0.08
69	133.5	D3			-30.1				
70	135	D3	3.7	-7.5	-29.2	32.9			
71	136	D3	5.6	-6.7	-27.8	33.4	-1.22	0.41	0.01
72	142	D4							
73	142.4	D4	-1.3	-0.9	-29.2	27.9	-0.44	0.95	0.04
74	156.5	D4	-1.1	-0.4	-28.1	27.0	-1.51	0.59	0.01
75	158	D4			-28.5				
76	166	D4			-26.1				
77	167	D4	0.4		-27.8	28.2	-3.41	0.1	0.18
78	172.2	D4	3.3	-1.8					
79	174	D4	4.7	-3.0	-27.1	31.8			
80	175.5	D4	4.9	-1.7	-28	32.9	-1.21	0.17	0.11
81	179.8	D4	5.2	-4.5	-27	32.2			
82	180	D4	5.4	-5.3	-25.6	31.0	-0.79	0.12	0.07
83	194	D4	1.8		-27.9	29.7			
84	203	DG	0.9	-2.8			-2.55	0.14	0.13
85	209	DG					-1.08	0.24	0.08
86	213	DG	3.3	-4.0			-2.19	0.10	0.07
87	217	DG	3.2	-3.4			-1.55	0.17	0.07

$\delta^{15}\text{N}^3$	N [wt. %]	TOC [wt.%]	C/N	ΣREE [$\mu\text{g/g}$]	Ce/Ce*4	$\text{Y}_\text{N}/\text{Ho}_\text{N}$	$\text{Pr}_\text{N}/\text{Yb}_\text{N}$	EF $\text{Mn}_{(\text{Cal-S})}$
4.6	0.051	0.21	4.1	8.8	1.4	1.3	0.83	2.9
5.3	0.137	0.97	7.1	44	1.16	1.5	0.75	2.1
5.4	0.126	0.89	7.1	11	0.98	1.6	0.7	2.4
3.1	0.015	0.59	39	3.9	0.98	1.3	1.07	1.2
3.1	0.015	0.59	39	3.5	1.09	1.4	0.84	3.5
5.0	0.029	0.11	3.9	14	1.33	1.4	1.32	
5.0	0.029	0.11	3.9	2.6	0.87	1.5	0.94	1.6
3.4	0.015	0.17	11	2.7	1.09	1.5	1	3.4
4.1	0.012	0.15	12	3.4	1.23	1.5	0.73	5.3
2.7	0.018	0.23	13	2.9	0.76	2.1	0.31	2.3
3.0	0.009	0.43	48	2.9	0.71	1.6	0.75	1.5
4.9	0.039	0.21	5.5	5.7	1.08	1.5	1.2	9.5
5.6	0.126	0.56	4.4	15	1.03	1.4	0.97	2.4
4.6	0.013	0.13	10	8.6	1.06	1.7	1.39	34
4.6	0.013		11	11	0.86	1.5	1.29	4.4
4.8	0.01	0.1	9.6	14	0.94	1.7	2.59	116
5.5	0.01	0.09	8.7	16	0.86	1.6	3.24	257
5.2	0.015	0.14	9.3	11	0.97	1.5	2.23	31
3.7	0.008			8.3	0.79	1.5	2.03	74
2.7	0.007	0.05	7.3	3.5	0.69	1.7	1.83	
3.6	0.010			3.0	0.7	1.8	1.23	
3.6	0.009	0.07	8.0	6.7	0.87	1.7	1.37	162
3.3	0.012	0.17	14.5	11	0.97	1.3	1.67	7
5.3	0.018	0.24	13.1	10	1.02	1.4	1.98	19
4.1	0.009			12	1.01	1.5	2.97	60
4.2	0.008	0.16	20	9.0	0.87	1.4	2.21	32
4.4	0.007	0.31	44	16	0.99	1.8	1.17	2
4.0	0.007	0.13	18	11	1.01	1.5	2.3	10
5.5	0.017			12	0.86	1.1	1.04	2.1
5.9	0.048	1.61	34	1.9	0.77	2.4	0.38	0.1
5.6	0.023	0.13	5.5	7.1	1.2	1.4	0.42	1.6
4.3	0.008	0.07	8.1	7.4	1.1	1.6	0.54	3.5
0.4	0.008	0.04	5.5	1.9	1.2	2.1	0.19	0.6
		0.02		0.99	0.7	2.7	0.23	0.2
4.1	0.01	0.18	18	9.1	0.69	1.3	0.87	2.7
5.1	0.022	0.09	4	14.5	0.64	1.3	1.4	4.3
3.3	0.008	0.03	3.3	11	0.67	1.3	1.7	2.6
1.7	0.005	0.14	29	13	0.75	1.4	2	1.9
		0.09		13	0.7	1.5	2	3.5
0.2	0.008	0.09	12					
				0.43	0.76	1.7	0.15	1.9
				0.56	0.86	1.6	0.2	5.7
				0.51	0.88	1.6	0.18	2.7
				0.69	0.83	1.8	0.23	2.5



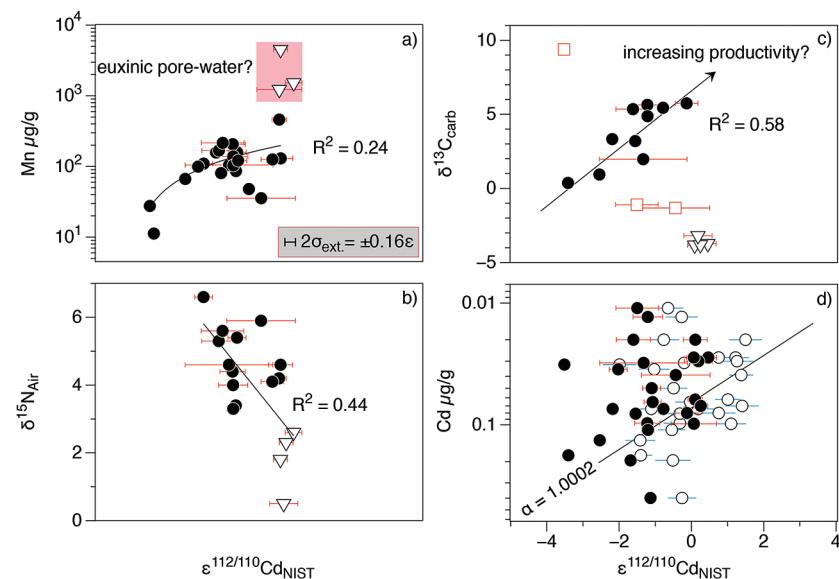


Figure 2 (a) Mn vs. $\epsilon^{112/110}\text{Cd}$. Cap dolomites (open triangles) have high Mn concentrations and exhibit positive $\epsilon^{112/110}\text{Cd}$. (b) N vs. Cd isotopic compositions reveal negative trend. (c) Carbon vs. Cd isotopic compositions show slight positive correlation when extreme values (red squares) and cap dolomites are excluded. (d) Cd concentrations vs. $\epsilon^{112/110}\text{Cd}$ values scatter along modern Southern Ocean fractionation line (Abouchami *et al.*, 2011), open circles represent coeval calculated $\epsilon^{112/110}\text{Cd}_{\text{sw}}$; note that the seawater Cd concentrations cannot be estimated from those measured in the carbonates.

As has been discussed above, there is still no consensus as to why cadmium is taken up by phytoplankton in the surface ocean, nor at which step (or steps) in this process the isotope fractionation takes place. Nevertheless, it is clear that $\epsilon^{112/110}\text{Cd}$ is a good indicator of biological productivity in the modern surface ocean: Cd uptake into OM leads to a depletion of light Cd in the photic zone. But can Cd isotopes in a marine sedimentary archive be used as a palaeo-productivity proxy? Under closed-system conditions (*e.g.*, a restricted basin) Ediacaran carbonates precipitating in biologically productive environments would be expected to have higher (heavier) $\epsilon^{112/110}\text{Cd}$ and $\delta^{13}\text{C}_{\text{carb}}$. The Xiaofenghe carbonates do exhibit a positive correlation between $\epsilon^{112/110}\text{Cd}$ and $\delta^{13}\text{C}_{\text{carb}}$ (Fig. 2c), consistent with increasing bio-productivity. However, this correlation only exists once light $\delta^{13}\text{C}_{\text{carb}}$ values from the basal Doushantuo (oxidation of a ^{12}C -enriched hydrocarbon source) and one sample with extremely heavy $\delta^{13}\text{C}_{\text{carb}}$ of +9 (presumably due to evaporation) are excluded.

The $\epsilon^{112/110}\text{Cd}$ and $\delta^{15}\text{N}$ curves in Figure 1 show an anti-correlation in some parts of the profile - for example, higher $\epsilon^{112/110}\text{Cd}$ in the cap dolomites with $\delta^{15}\text{N}$ having low but positive values (Fig. 2b). This trend would be consistent with

strong N_2 fixation by diazotrophs in the euphotic zone (Sachs and Repeta, 1999). Cyanobacteria blooms of this sort are often documented from redox-stratified basins (Struck *et al.*, 2004), and recent work by Georgiev *et al.* (2015) has highlighted the redox control on Cd distribution in late Permian marine sediments. Cd is not a redox-sensitive element *per se*, but Cd bound to OM will become enriched in anoxic sediments whenever oxidation of OM is inhibited.

Cadmium may also be co-precipitated with sulphides under euxinic conditions (Framson and Leckie, 1978), such as prevail in the deeper parts of the Black Sea today, where Cd is removed almost quantitatively from the water column and enriched in bottom sediments (Lewis and Landing, 1992). The effect of authigenic sulphides on Cd isotope fractionation is still not well understood. Cadmium isotope data on hydrothermal sulphide ores (Schmitt *et al.*, 2009; Wen *et al.*, 2016) and quantum chemical calculations (Yang *et al.*, 2015) suggest that the light isotopes of Cd would be preferentially bound into the sulphide phase. On the other hand, Rolison *et al.* (2015) did not find the high $\epsilon^{112/110}\text{Cd}$ in the deeper parts of the Black Sea water column that one would expect. All in all this means that sulphide-bearing anoxic sediments should most likely have higher Cd concentrations and more negative $\epsilon^{112/110}\text{Cd}$ than those of oxic surface waters.

In the Xiaofenghe carbonates, Mn enrichments correlate with high $\epsilon^{112/110}\text{Cd}$ (Fig. 2a). As Mn in oxic waters is usually incorporated into Mn oxyhydroxides, such enrichments are likely to reflect reduction of Mn to the 2+ state at the anoxic pore-water sediment interface and subsequent incorporation into CaCO_3 (Thomson *et al.*, 1986). The cap dolomites exhibit Mn enrichments, more positive $\epsilon^{112/110}\text{Cd}$ and low Cd concentrations. Furthermore, sedimentary sulphides ranging from 10 to 40 μm in size are abundant in thin section (see Fig. S-2). The fact that Ce anomalies are negative ($\text{Ce}/\text{Ce}^* < 0.9$) in shallow Yangtze Platform cap dolomites (Fig. 1h) suggests that early Ediacaran surface-waters were already oxic; nonetheless, pore-waters may still have been anoxic, leading to the formation of sulphides and Mn-rich carbonates. In summary, incorporation of light Cd into sulphides may raise $\epsilon^{112/110}\text{Cd}$ in associated carbonates, and might have affected the Xiaofenghe cap dolomites.

Experiments on precipitation of inorganic calcite from seawater by Horner *et al.* (2011) show that the seawater/calcite fractionation factor for Cd is insensitive to temperature, Mg concentration and precipitation rate. By contrast, precipitation of calcites from freshwater does not lead to any Cd isotopic fractionation, presumably as a result of ion blocking on mineral surface sites. Since these experiments by Horner *et al.* (2011) used only seawater and freshwater end-members, we will assume to first order that Cd isotope fractionation into calcite depends linearly on salinity. Using Y/Ho ratios as an indicator of palaeo-salinity we are then able to calculate $\epsilon^{112/110}\text{Cd}$ for seawater in equilibrium with the Xiaofenghe carbonates (see Fig. S-3 for more details). The resulting $\epsilon^{112/110}\text{Cd}_{\text{sw}}$ range between -2 and +1.5 (Fig. 1e), which is still slightly lower than the lower bound of modern surface seawater $\epsilon^{112/110}\text{Cd}$ but scatter around the Rayleigh fractionation line defined by modern Southern Ocean seawaters (Abouchami *et al.*, 2011; Fig. 2d). If the Cd



isotopic variations observed are controlled by changes in seawater salinity at the Xiaofenghe depositional site, estuarine mixing of seawater and river water, as described in Hohl *et al.* (2015), may account for the observed variation. The correlation between Y/Ho and $\epsilon^{112/110}\text{Cd}$ (see Fig. 1g and Fig. S-1c) may therefore be due to an increased riverine input, flattening the REE patterns, decreasing the total salinity and thus reducing the isotopic fractionation into calcite. Any further increase in riverine input would most likely drown out any potential biological signal in the stable isotope proxies, such as $\epsilon^{112/110}\text{Cd}$, which would then resemble typical crustal values.

Implications

Stable Cd isotopic compositions of Ediacaran-age carbonates from the Xiaofenghe section on the Yangtze Platform show significant variations of up to four $\epsilon^{112/110}\text{Cd}$ units. There are several possible reasons for these variations: part of the signal may be biological in origin while abiological (inorganic) processes almost certainly play a role as well. Factors controlling the Cd isotopic compositions may include fluid flow alteration, the precipitation of authigenic sulphides under anoxic pore water conditions, both processes possibly modifying $\epsilon^{112/110}\text{Cd}$ in the cap dolomites; additionally there are changes in Cd isotope fractionation into calcite as a function of salinity, as suggested here for the upper Doushantuo. Encouragingly, our salinity-corrected palaeo-seawater $\epsilon^{112/110}\text{Cd}_{\text{sw}}$ signals overlap those of modern surface waters. A positive correlation between $\delta^{13}\text{C}_{\text{carb}}$ and $\epsilon^{112/110}\text{Cd}$ is observed, which suggests that the Cd isotope fractionation might, in part, have a biological origin, meaning that phytoplankton were present as early as the Ediacaran. Future research on marine sediments will need to address the abiotic fractionation processes above, and correct for them, in order to arrive at any biologically-derived Cd isotope signal present.

Acknowledgements

This work was funded as part of DFG Research Group FOR-736 “The Precambrian-Cambrian Biosphere Revolution” (Subproject Be 1820/4-2). We thank Reimund Jotter and Wafa Abouchami at MPIC for discussions and their support in the lab, and members of FOR-736 who helped in sampling. We acknowledge helpful comments by Michael Tatzel, two anonymous reviewers and the editor, Helen Williams.

Editor: Helen Williams

Additional Information

Supplementary Information accompanies this letter at www.geochemicalperspectivesletters.org/article1704

Reprints and permission information is available online at <http://www.geochemicalperspectivesletters.org/copyright-and-permissions>

Cite this letter as: Hohl, S.V., Galer, S.J.G., Gamper, A., Becker, H. (2017) Cadmium isotope variations in Neoproterozoic carbonates - A tracer of biologic production? *Geochem. Persp. Let.* 3, 32-44.

References

- ABOUCAMI, W., GALER, S.J.G., DE BAAR, H.J.W., ALDERKAMP, A.C., MIDDAG, R., LAAN, P., FELDMANN, H., ANDREAE, M.O. (2011) Modulation of the Southern Ocean cadmium isotope signature by ocean circulation and primary productivity. *Earth and Planetary Science Letters* 305, 83–91.
- ADER, M., SANSJOFRE, P., HALVERSON, G.P., BUSIGNY, V., TRINDADE, R.I.F., KUNZMANN, M., NOGUEIRA, A.C.R. (2014) Ocean redox structure across the Late Neoproterozoic Oxygenation Event: A nitrogen isotope perspective. *Earth and Planetary Science Letters* 396, 1–13.
- BAU, M., DULSKI, P., MÖLLER, P. (1995) Yttrium and holmium in South Pacific seawater: vertical distribution and possible fractionation mechanisms. *Oceanographic Literature Review* 42, 955.
- BEBOUT, G.E., FOGEL, M.L. (1992) Nitrogen-isotope compositions of metasedimentary rocks in the Catalina Schist, California: Implications for metamorphic devolatilization history. *Geochimica et Cosmochimica Acta* 56, 2839–2849.
- BOYLE, E.A., SCLATER, F., EDMOND, J.M. (1976) On the marine geochemistry of cadmium. *Nature* 263, 42–44.
- BRAND, U., VEIZER, J. (1980) Chemical diagenesis of a multicomponent carbonate system-1: trace elements. *Journal of Sedimentary Petrology* 50, 1219–1236.
- CANFIELD, D.E., GLAZER, A.N., FALKOWSKI, P.G. (2010) The evolution and future of earth's nitrogen cycle. *Science* 330, 192–196.
- FRAMSON, P.E., LECKIE, J.O. (1978) Limits of coprecipitation of cadmium and ferrous sulfides. *Environmental Science and Technology* 12, 465–469.
- GEORGIEV, S.V., HORNER, T.J., STEIN, H.J., HANNAH, J.L., BINGEN, B., REHKÄMPER, M. (2015) Cadmium isotopic evidence for increasing primary productivity during the Late Permian anoxic event. *Earth and Planetary Science Letters* 410, 84–96.
- HALVERSON, G.P., HURTGEN, M.T. (2007) Ediacaran growth of the marine sulfate reservoir. *Earth and Planetary Science Letters* 263, 32–44.
- HORNER, T.J., SCHÖNBÄCHLER, M., REHKÄMPER, M., NIELSEN, S.G., WILLIAMS, H., HALLIDAY, A.N., XUE, Z., HEIN, J.R. (2010) Ferromanganese crusts as archives of deep water Cd isotope compositions. *Geochemistry, Geophysics, Geosystems* 11, 1–10.
- HORNER, T.J., RICKABY, R.E.M., HENDERSON, G.M. (2011) Isotopic fractionation of cadmium into calcite. *Earth and Planetary Science Letters* 312, 243–253.
- HOHL, S.V., BECKER, H., GAMPER, A., JIANG, S.-Y., WIECHERT, U., YANG, J.-H., WEI, H.-Z. (2015) Secular changes of water chemistry in shallow-water Ediacaran ocean: Evidence from carbonates at Xiaofenghe, Three Gorges area, Yangtze Platform, South China. *Precambrian Research* 270, 50–79.



- ISHIKAWA, T., UENO, Y., SHU, D., LI, Y., HAN, J., GUO, J. (2013) The $\delta^{13}\text{C}$ excursions spanning the Cambrian explosion to the Canglangpuian mass extinction in the Three Gorges area, South China. *Gondwana Research* 25, 1045–1056.
- KAUFMAN, A.J., KNOLL, A.H. (1995) Neoproterozoic variations in the C-isotopic composition of seawater: stratigraphic and biogeochemical implications. *Precambrian Research* 73, 27–49.
- KNOLL, A.H. (2015) Life on a Young Planet: The First Three Billion Years of Evolution on Earth. Princeton University Press.
- LACAN, F., FRANCOIS, R., JI, Y., SHERREL, R.M. (2006) Cadmium isotopic composition in the ocean. *Geochimica et Cosmochimica Acta* 70, 5104–5118.
- LAWRENCE, M.G., KAMBER, B.S. (2006) The behaviour of the rare earth elements during estuarine mixing—revisited. *Marine Chemistry* 100, 147–161.
- LEWIS, B.L., LANDING, W.M. (1992) The investigation of dissolved and suspended-particulate trace metal fractionation in the Black Sea. *Marine Chemistry* 40, 105–141.
- PARK, H., SONG, B., MOREL, F.M.M. (2007) Diversity of the cadmium-containing carbonic anhydrase in marine diatoms and natural waters. *Environmental Microbiology* 9, 403–413.
- PLANAVSKY, N., BEKKER, A., ROUXEL, O.J., KAMBER, B., HOFMANN, A., KNUDSEN, A., LYONS, T.W. (2010) Rare Earth Element and yttrium compositions of Archean and Paleoproterozoic Fe formations revisited: New perspectives on the significance and mechanisms of deposition. *Geochimica et Cosmochimica Acta* 74, 6387–6405.
- PRICE, N.M., MOREL, F.M.M. (1990) Cadmium and cobalt substitution for zinc in a marine diatom. *Nature* 344, 658–660.
- RIPPERGER, S., REHKÄMPER, M., PORCELLI, D. (2007) Cadmium isotope fractionation in seawater - a signature of biological activity. *Earth and Planetary Science Letters* 261, 670–684.
- ROLISON, J.M., STIRLING, C.H., GEORGE, E., MIDDAG, R., GAULT-RINGOLD, M., RIJKENBERG, M.J.A., DE BAAR, H.J.W. (2015) Biogeochemical cycling of the uranium, iron and cadmium isotope systems during oceanic anoxia: A case study of the Black Sea. *Goldschmidt Abstracts* 2015, 2671.
- SACHS, J.P., REPETA, D.J. (1999) Oligotrophy and Nitrogen Fixation During Eastern Mediterranean Sapropel Events. *Science* 286, 2845–2848.
- SCHMITT, A.-D., GALER, S.J.G., ABOUCHAMI, W. (2009) Mass-dependent cadmium isotopic variations in nature with emphasis on the marine environment. *Earth and Planetary Science Letters* 277, 262–272.
- STRUCK, U., POLLEHNE, F., BAUERFEIND, E., BODUNGEN, VON B. (2004) Sources of nitrogen for the vertical particle flux in the Gotland Sea (Baltic Proper) - results from sediment trap studies. *Journal of Marine Systems* 45, 91–101.
- THOMSON, J., HIGGS, N.C., JARVIS, I., HYDES, D.J. (1986) The behaviour of manganese in Atlantic carbonate sediments. *Geochimica et Cosmochimica Acta* 50, 1807–1818.
- WASYLENKI, L.E., SWIHART, J.W., ROMANIELLO, S.J. (2014) Cadmium isotope fractionation during adsorption to Mn oxyhydroxide at low and high ionic strength. *Geochimica et Cosmochimica Acta* 140, 212–226.
- WEN, H., ZHU, C., ZHANG, Y., CLOQUET, C., FAN, H., FU, S. (2016) Zn/Cd ratios and cadmium isotope evidence for the classification of lead-zinc deposits. *Scientific Reports* 6, 25273, doi: 10.1038/srep25273.
- XIAO, S., MCFADDEN, K.A., PEEK, S., KAUFMAN, A.J., ZHOU, C., JIANG, G., HU, J. (2012) Integrated chemostratigraphy of the Doushantuo Formation at the northern Xiaofenghe section (Yangtze Gorges, South China) and its implication for Ediacaran stratigraphic correlation and ocean redox models. *Precambrian Research* 192–195, 125–141.
- YANG, J., LI, Y., LIU, S., TIAN, H., CHEN, C., LIU, J., SHI, Y. (2015) Theoretical calculations of Cd isotope fractionation in hydrothermal fluids. *Chemical Geology* 391, 74–82.
- YIN, L., ZHU, M., KNOLL, A.H., YUAN, X., ZHANG, J., HU, J. (2007) Doushantuo embryos preserved inside diapause egg cysts. *Nature* 446, 661–663.

■ Cadmium isotope variations in Neoproterozoic carbonates – A tracer of biologic production?

S.V. Hohl^{1,2*}, S.J.G. Galer³, A. Gamper⁴, H. Becker¹

■ Supplementary Information

The Supplementary Information includes:

- Geologic Background, Sample Selection and Analytical Methods
- Supplementary Figures S-1 to S-3
- Supplementary Information References

Geologic Background, Sample Selection and Analytical Methods

The Xiaofenghe section was sampled in detail with the aim of determining the geochemical variations in carbonate sediments and to study the role of alteration and preservation of primary compositions. The samples were carefully selected in the field and later pre-screened using a petrographic microscope and SEM to avoid samples with alteration structures, such as calcitic veins or weathering fronts. The samples were then cleaned with deionised water and powdered. Major and trace element compositions of acetic acid leachates and Sr-Nd-C_{carb}-O_{carb} isotopic compositions have been reported in Hohl *et al.* (2015).

Stable isotope ratios and concentrations of nitrogen and organic carbon were obtained using a Thermo-Finnigan MAT V isotope ratio mass spectrometer coupled to a Thermo Flash EA 1112 elemental analyser via a Thermo/Finnigan ConFlo III-interface at the Museum für Naturkunde in Berlin. $\delta^{15}\text{N}$ analyses were performed on the bulk rock powder whereas for $\delta^{13}\text{C}_{\text{org}}$ measurements, sample powders were decalcified before analysis using 2 M HCl. Isotope ratios

1. Institut für Geologische Wissenschaften, Freie Universität Berlin, Germany
2. State Key Laboratory for Mineral Deposits Research, Department of Earth Sciences, Nanjing University, Nanjing, China
- * Corresponding author (email: shohl@zedat.fu-berlin.de)
3. Max-Planck-Institut für Chemie, Abteilung Klimageochemie, Mainz, Germany
4. Museum für Naturkunde Berlin, Leibniz Institute for Evolution and Biodiversity Science, Berlin, Germany



are expressed in the conventional delta notation relative to AIR (nitrogen) and the V-PDB (Vienna PeeDee Belemnite) standard (carbon), respectively. The standard deviation for repeated measurements of a laboratory standard material (peptone) is generally better than 0.2 ‰ for both isotopic systems. After sample combustion, a CO₂ trap was used to reduce interferences between bulk rock nitrogen and carbon isotope signals.

Stable Cd isotope analyses were undertaken on leachates of the carbonate fraction so as to avoid any detrital material. We reacted 1 g of sample powder in pre-cleaned 50 mL centrifuge tubes with 50 mL of 1 M acetic acid-ammonium acetate buffer (pH = 5) at room temperature under continuous rotation overnight. The solution was centrifuged and the supernatant pipetted out. Aliquots of the leachate containing ~100 ng Cd were taken and optimal amounts of ¹⁰⁶Cd-¹⁰⁸Cd double-spike solution added, as described in Schmitt *et al.* (2009). After equilibration with the spike, 0.6 mL of 8.5 M HBr per 10 mL sample solution was added to obtain a concentration of ~0.5 N HBr. The Cd separation and purification used a two-step procedure: first, the solutions containing Cd were passed through BioRad Polyrep columns filled with 200 µL of BioRad AG1-X8 anion-exchange resin (100-200 mesh) in nitrate form to retain the Cd. The resin was rinsed repeatedly with 1 N HCl (to remove traces of bromide and matrix) followed by elution of the Cd with 0.25 N HNO₃. For purification, the Cd eluted was again acidified to ~0.5 N HBr and passed a second time through the column.

The samples were then loaded onto single Re filaments, covered with 1 µL silica gel-phosphoric acid activator and dried. Cadmium isotopic compositions were measured on a Triton (ThermoFisher) Thermal Ionisation Mass Spectrometer (TIMS) at the Max-Planck-Institut für Chemie in Mainz operating in static multi-collection mode. Running temperatures were ~1150 °C. Data reduction for the natural and instrumental mass-dependent isotope fractionation used the double-spike algorithm assuming an exponential fractionation law; the statistical uncertainties are based on reducing each measurement cycle (8 seconds) during the run. The ¹⁰⁶Cd-¹⁰⁸Cd double spike was originally calibrated against an in-house JMC Cd Plasma solution (Lot: 15922032), assuming ¹¹⁰Cd/¹¹²Cd = 0.520089 (Rosman *et al.*, 1980) for unspiked cadmium.

The Cd isotope data are expressed as ε^{112/110}Cd values (deviations of ¹¹²Cd/¹¹⁰Cd in parts per 10,000 from a reference material):

$$\epsilon^{112/110}Cd = \left[\frac{^{110}Cd/^{112}Cd_{RM}}{^{110}Cd/^{112}Cd_{sample}} - 1 \right] \times 10^4 \quad \text{Eq. S-1}$$

As reference material (RM) for “zero delta” we used the NIST SRM 3108 Cd standard (Lot: 130116), measured absolutely as ¹¹⁰Cd/¹¹²Cd = 0.520121 ± 0.000004 (Abouchami *et al.*, 2012). The long-term external reproducibility on ε^{112/110}Cd is ±0.16 ε unit at the 2s level (2 SD). Cadmium concentrations were obtained by isotope dilution from the bias-corrected ¹⁰⁶Cd/¹¹²Cd and have analytical uncertainties of less than 0.1 % (2 RSD).

Supplementary Figures

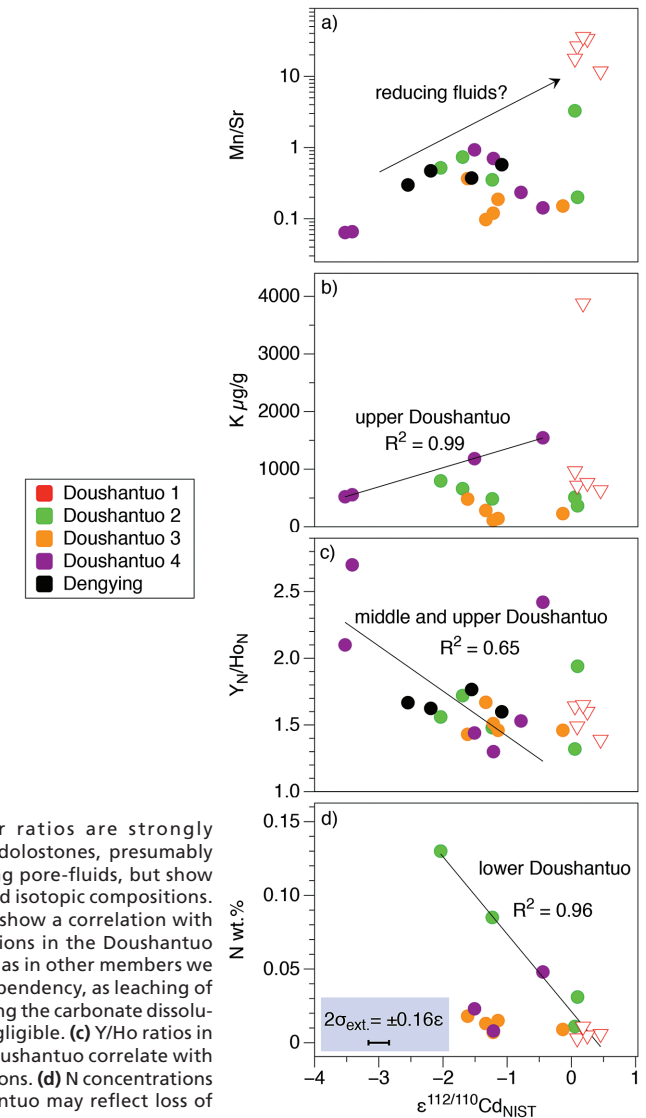


Figure S-1 (a) Mn/Sr ratios are strongly elevated in the cap dolostones, presumably as a result of reducing pore-fluids, but show no correlation with Cd isotopic compositions. (b) K concentrations show a correlation with Cd isotope compositions in the Doushantuo IV member, however as in other members we do not report any dependency, as leaching of detrital minerals during the carbonate dissolution is considered negligible. (c) Y/Ho ratios in middle and upper Doushantuo correlate with Cd isotopic compositions. (d) N concentrations in the lower Doushantuo may reflect loss of N during diagenesis.



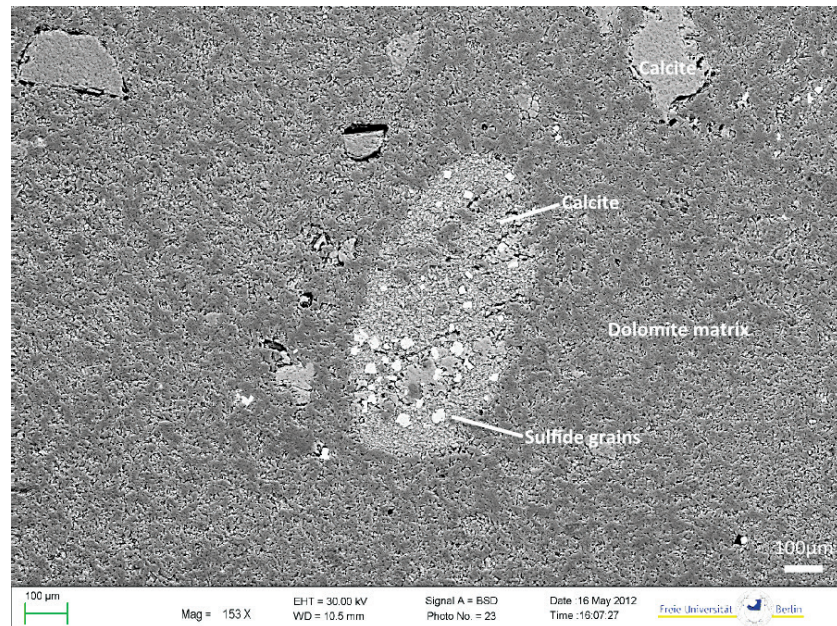


Figure S-2 BSD picture of a Xiaofenghe section cap dolostone at 2.35 m stratigraphic height. The sample shows calcitic fillings within a formerly porous dolomitic matrix. Subhedral (10-40 μm diameter) authigenic sulphide grains are abundant in samples from the basal Doushantuo cap dolostones. Scale bar is 100 μm .

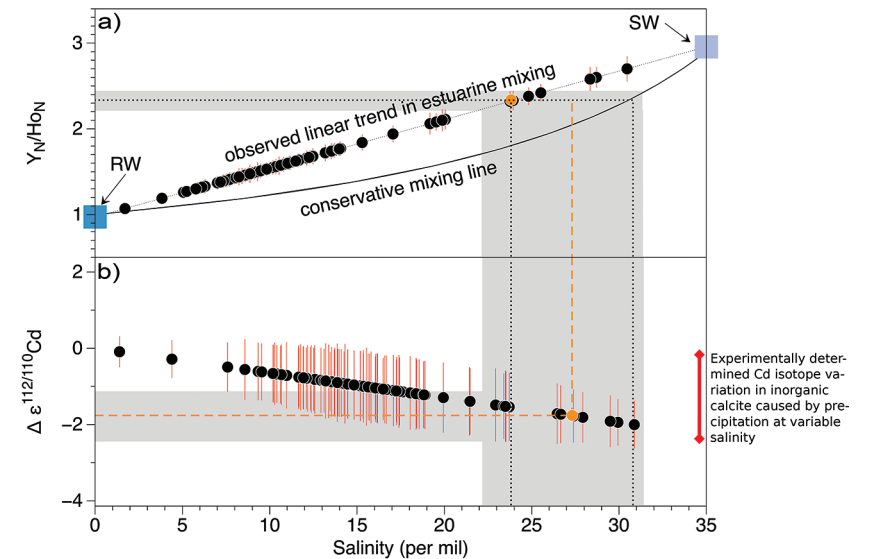


Figure S-3 (a) Assuming that fractionation of Cd into carbonate phases is salinity controlled, we used Y/Ho ratios in acetic acid leachates as a record for salinity variations. In modern estuarine mixing environments shale normalised Y/Ho ratios vary from 0.97 for river water (RW) to 2.96 for seawater (SW) (Lawrence and Kamber, 2006), confirmed by similar Y/Ho ranges obtained by other authors (e.g., Bau and Dulski, 1995). We used these two values as end members for the calculation of the corrected Ediacaran Cd isotope curve (Fig. 1e). A general 5 % uncertainty (2 RSD) was applied on the trace element concentration data. We calculated salinities for a case in which salinity and Y/Ho are linearly correlated (dotted line) and another case in which the correlation follows a conservative mixing line between the two end members (bold line). The average of the two cases (exemplified by the dashed orange line) was then used to calculate model salinity values. (b) From calculated salinities S we inferred $\epsilon^{112/110}\text{Cd}$ shifts that result from Cd isotopic fractionation under variable salinity as shown experimentally by (Horner *et al.*, 2011). Following their work, we assume a linear relationship between no shifts at $S = 0$ ‰ and a shift of $-2.27 \epsilon^{112/110}\text{Cd}$ at $S = 35$ ‰ ($\alpha_{\text{CaCO}_3-\text{Cd}_{\text{aq}}} = 0.9995773 \pm 0.00006$). Finally, with this information we were able to calculate a salinity independent $\epsilon^{112/110}\text{Cd}$ curve of seawater that may have been in equilibrium with the carbonates at the time of their precipitation (Fig. 1e).

Supplementary Information References

- ABOUCAMI, W., GALER, S.J.G., HORNER, T.J., REHKÄMPER, M., WOMBACHER, F., XUE, Z. (2012) A Common Reference Material for Cadmium Isotope Studies - NIST SRM 3108. *Geostandards and Geoanalytical Research* 37, 5–17.
- BAU, M., DULSKI, P. (1995) Comparative study of yttrium and rare-earth element behaviours in fluorine-rich hydrothermal fluids. *Contributions to Mineralogy and Petrology* 119, 213–223.
- HOHL, S.V., BECKER, H., GAMPER, A., JIANG, S.-Y., WIECHERT, U., YANG, J.-H., WEI, H.-Z. (2015) Secular changes of water chemistry in shallow-water Ediacaran ocean: Evidence from carbonates at Xiaofenghe, Three Gorges area, Yangtze Platform, South China. *Precambrian Research* 270, 50–79.



- HORNER, T.J., RICKABY, R.E.M., HENDERSON, G.M. (2011) Isotopic fractionation of cadmium into calcite. *Earth and Planetary Science Letters* 312, 243–253.
- LAWRENCE, M.G., KAMBER, B.S. (2006) The behaviour of the rare earth elements during estuarine mixing—revisited. *Marine Chemistry* 100, 147–161.
- ROSMAN, K.J.R., DE LAETER, J.R., GORTON, M.P. (1980) Cadmium isotope fractionation in fractions of two H3 chondrites. *Earth and Planetary Science Letters* 48, 166–170.
- SCHMITT, A.-D., GALER, S.J.G., ABOUCHAMI, W. (2009) High-precision cadmium stable isotope measurements by double spike thermal ionisation mass spectrometry. *Journal of Analytical Atomic Spectrometry* 24, 1079.

